4H-Silicon Carbide p-n Diode for Harsh Environment Sensing Applications

Shiqian Shao

Electrical Engineering and Computer Sciences
University of California at Berkeley

Technical Report No. UCB/EECS-2016-31
http://www.eecs.berkeley.edu/Pubs/TechRpts/2016/EECS-2016-31.html

May 1, 2016

Copyright © 2016, by the author(s).
All rights reserved.

Permission to make digital or hard copies of all or part of this work for personal or classroom use is granted without fee provided that copies are not made or distributed for profit or commercial advantage and that copies bear this notice and the full citation on the first page. To copy otherwise, to republish, to post on servers or to redistribute to lists, requires prior specific permission.

4H-Silicon Carbide p-n Diode for Harsh Environment Sensing Applications

by

Shiqian Shao

A thesis submitted in partial satisfaction of the

requirements for the degree of

Master of Science

in

Engineering - Electrical Engineering and Computer Sciences

in the

Graduate Division

of the

University of California, Berkeley

Committee in charge:

Professor Albert P. Pisano, Chair
Professor Tsu-Jae King Liu

Spring 2015

4H-Silicon Carbide p-n Diode for Harsh Environment Sensing Applications

Copyright © 2015

by

Shiqian Shao

4H-Silicon Carbide p-n Diode for Harsh Environment Sensing Applications

by Shiqian Shao

Research Project

Submitted to the Department of Electrical Engineering and Computer Sciences, University of California at Berkeley, in partial satisfaction of the requirements for the degree of **Master of Science, Plan II**.

Approval for the Report and Comprehensive Examination:

Committee:

____

Professor Albert P. Pisano
Research Advisor

____

(Date)

* * * * * * *

____

Professor Tsu-Jae King Liu
Second Reader

____

(Date)

Abstract

4H-Silicon Carbide p-n Diode for Harsh Environment Sensing Applications

by

Shiqian Shao

Master of Science in Electrical Engineering and Computer Science

University of California, Berkeley

Professor Albert P. Pisano, Chair

A harsh environment usually involves one or more of the following: extreme temperature, high pressure, high shock, high radiation, and chemical attack. High temperature electronics and sensors that are able to operate between 300 °C to 600 °C have drawn a lot of attention due to their wide applications in harsh environment such as in oil/gas exploration, geothermal development, industrial manufacturing processes, and space exploration. Silicon carbide (SiC) has become a great candidate as an electrical material for these harsh environment applications because of its wide bandgap, its high temperature operation ability, its excellent thermal and chemical stability, and its high breakdown electric field strength. In this work, the stable performance of 4H-SiC p-n diodes from room temperature to 600 °C has been demonstrated. Simulation, fabrication and characterization of the 4H-SiC p-n diodes are performed. The simulated 4H-SiC p-n diode shows that its turn-on voltage changes from 2.7 V to 1.45 V when temperature increases from 17 ºC to 600 ºC. The fabricated 4H-SiC p-n diode has a turn-on voltage from 2.6 V to 1.3 V with temperature rising from 17 ºC to 600 ºC, which are in good agreement with the simulation results. The demonstration of the stable operation of the 4H-SiC p-n diodes at high temperature up to 600 ºC shows great potentials for 4H-SiC devices and circuits working in harsh environment electronic and sensing applications.

To my family

Contents

Contents i

List of Figures ii

List of Tables iv

1. Introduction 1

1.1 Harsh Environment Sensing Applications 1

1.2 Material Selection — 4H-Silicon Carbide....................2

1.3 4H-SiC Extreme-temperature Low-power Applications....................5

1.4 Research Objective and Thesis Overview....................6

2. Material and Device Physics from Room to Extreme Temperature 7

2.1 Temperature-dependent Coefficients of 4H-Silicon Carbide....................7

2.2 Device Physics of 4H-SiC p-n Diode 9

3. Fabrication of 4H-SiC p-n Diode 13

3.1 Fabrication Process of 4H-SiC p-n Diode 13

3.2 Fabricated 4H-SiC p-n Diode and Characterization Platform 16

4. Device Performance and Temperature Sensing Applications of 4H-SiC p-n Diode 18

4.1 Device Performance of 4H-SiC p-n Diode from room to Extreme Temperature 18

4.2 Temperature Sensing Application of 4H-SiC p-n Diode 21

5. Conclusion and Future Work 23

5.1 Conclusion 23

5.2 Future Work 23

References 25

List of Figures

Figure 1.1 Five harsh environment application examples including the peak temperature in the sensing ambient and the typical sensing functions required for each application Introduction……………………………………………………………………………………2

Figure 1.2 The tetrahedron structure of SiC crystal…..……………..……………..……3

Figure 1.3 Three types of bilayers seen along c-axis…..……………………………..……3

Figure 1.4 Stacking orders of bilayers in [11$\underline{2}$0] plane for 3C-SiC, 2H-SiC, 4H-SiC and 6H-SiC. ……………………………………………………………………………………3

Figure 2.1 4H-SiC energy bandgap versus temperature...………………………………8

Figure 2.2 Intrinsic carrier concentrations of silicon and 4H-SiC versus temperature....8

Figure 2.3 The simulated current-voltage plots of 4H-SiC p-n diode from room temperature to 600 °C…………………………..……….……………………………12

Figure 3.1 Starting wafer for the 4H-SiC p-n diode fabrication process………………13

Figure 3.2 (a) Top view schematic of the 4H-SiC p-n diode; (b) cross-sectional view schematic of the 4H-SiC p-n diode at the red line in (a)…………………..……………14

Figure 3.3 (a) Starting wafer: single crystal 4H-SiC wafer with four epitaxial layers; (b) first SiC etching to expose the n^+ contact layer; (c) second SiC etching to isolate single diode; (d) oxide passivation deposition and patterning; (e) n-type metal liftoff and annealing; (f) p-type metal liftoff and annealing………………………...……………15

Figure 3.4 The optical microscopic image of the fabricated 4H-SiC p-n diode with a 200 μm diameter circular junction.…………………………………...………….……16

Figure 3.5 The high temperature probe station including hot chunk, thermal heater, and water cooler.………………………………………………………………………17

Figure 4.1 The testing results of 4H-SiC p-n diode from room temperature to 600 °C..19

Figure 4.2 The testing results of 4H-SiC p-n diode from room temperature to 600 °C in a semi-log plot…………………………………………………………………….....19

Figure 4.3 Comparison of the simulation and testing results of the 4H-SiC p-n diode from room temperature to 600 °C. (a) Comparison of turn-on voltage; (b) comparison of the on-resistance……………………………………………………………………..20

Figure 4.4 The temperature sensing demonstration of 4H-SiC p-n diode from room temperature to 600 °C at 1 mA current………………………………………………..21

Figure 4.5 The temperature sensing demonstration of 4H-SiC p-n diode from room temperature to 600 °C at 0.1 μA current………………………………………………22

List of Tables

Table 1.1 Electrical, mechanical and optical properties of silicon and wide bandgap materials. (*values perpendicular to the c-axis.)…………………………..………………4

Table 1.2 Electronic requirements for harsh environment sensing applications in industrial gas turbine and geothermal well.……………...………………..………………5

Chapter 1

Introduction

1.1 Harsh Environment Sensing Applications

Recently, harsh environment electronics and sensors have drawn much attention in both research and industrial fields [1, 2]. Application examples for such harsh environment are in oil & gas exploration, in geothermal well power plant development, in automotive engines and aircraft engines, in industrial gas turbines, in industrial manufacturing process and in space exploration [3-5]. In-situ real-time monitoring is very promising for high efficiency, high operating accuracy, long lifetime, low cost and safe operation in the harsh environments aforementioned. Wireless techniques are especially useful for telemetry harsh environment sensing applications such as gas turbine blade status monitoring, deep well oil drilling guidance or subsurface environment exploration in geothermal power plants [6]. However, the harsh environment usually involves one or more of the following: extreme temperature, high pressure, high shock, high radiation, and chemical attack, which are major challenges for electronics and sensors [7-9].

In electronics nowadays, silicon has been widely used due to its high quality, stable oxide and low cost. However, it is not a suitable semiconductor material for harsh environments especially in the extreme high temperature aspect. The intrinsic carrier concentration of silicon is approximately 2×10^{16} cm^{-3} at 300 °C, which makes it difficult to form doping gradient for well functional microelectronic devices. Meanwhile, its elastic modulus declines above 600 °C, which degrades its mechanical performance for micro electro mechanical system (MEMS) sensing devices [10]. New materials are necessary to be explored for extreme temperature harsh environment applications such as in automobile engines, underground exploration for oil, gas & geothermal energy, and industrial gas turbines. Wide bandgap materials have been proposed for these extreme temperature harsh environment sensing applications because of its low intrinsic carrier concentration and good mechanical performance at high temperature and its high thermal conductivity which is able to reduce self-heating effect [11].

For integrated multifunctional harsh environment sensing systems, the blocks of

different sensing functions such as temperature sensor, pressure sensor, accelerometer, strain sensor, chemical sensor are desired for different harsh environment applications [11, 12]. Figure 1.1 shows some harsh environment application examples including the peak temperature in the sensing ambient and the typical sensing functions required for each application. As indicated in Figure 1.1, sensors and electronic devices working at extreme temperature from 300 °C to 600 °C are very promising for plenty of harsh environment applications and it is still a major challenge for them, too.

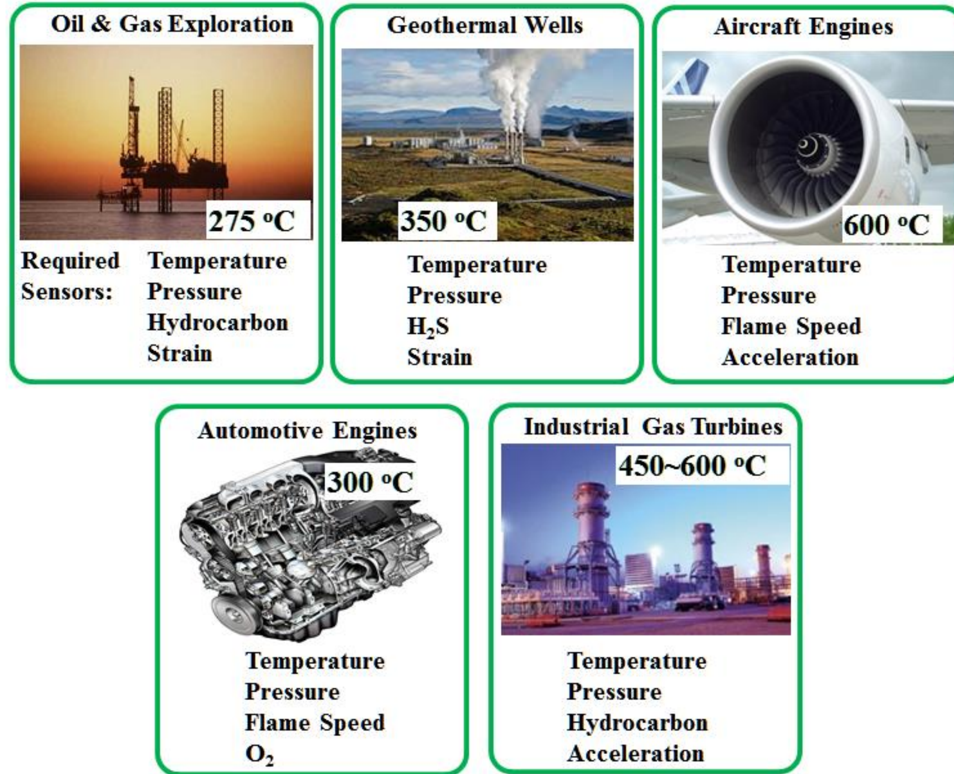

Figure 1.1 Five harsh environment application examples including the peak temperature in the sensing ambient and the typical sensing functions required for each application.

1.2 Material Selection — 4H-Silicon Carbide

Silicon carbide (SiC) has been employed as ceramic, electrical, mechanical, optoelectronic materials and many others since it was discovered in 19th century [13]. There are about 250 crystal structures of silicon carbide. The most common structures are 3C-SiC, 4H-SiC and 6H-SiC. In a silicon carbide unit cell, Along with c-axis, each

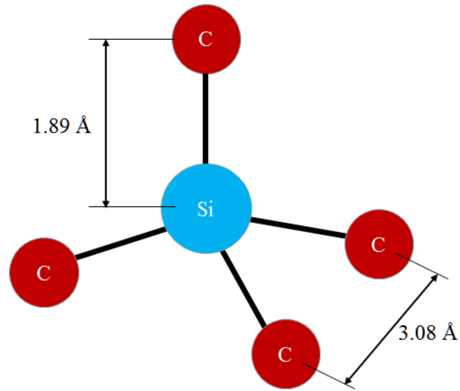

Figure 1.2 The tetrahedron structure of SiC crystal.

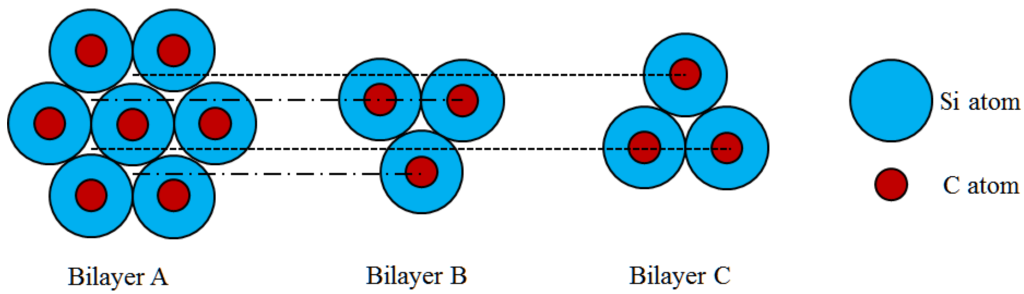

Figure 1.3 Three types of bilayers seen along c-axis.

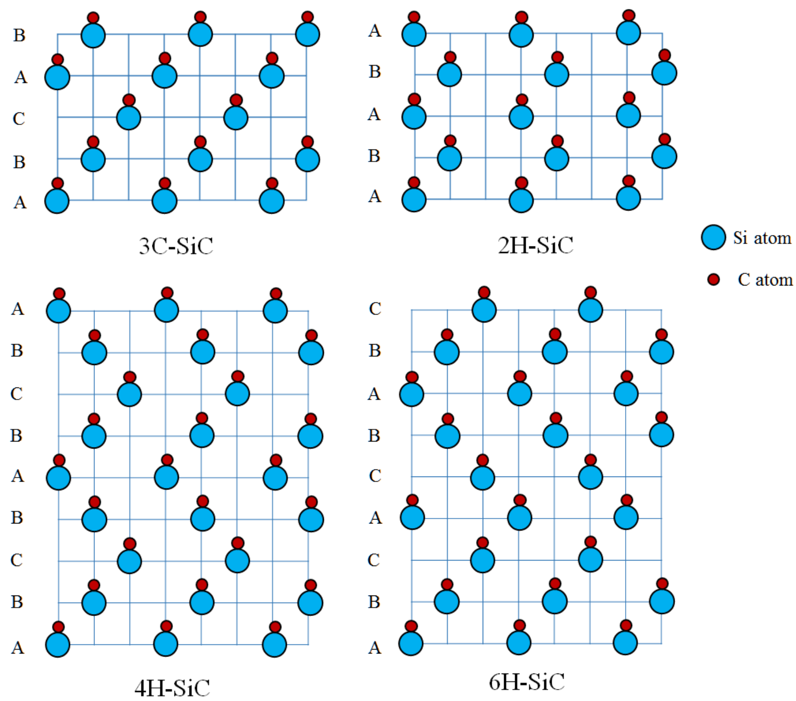

Figure 1.4 Stacking orders of bilayers in [11$\underline{2}$0] plane for 3C-SiC, 2H-SiC, 4H-SiC and 6H-SiC.

	Si	3C-SiC	4H-SiC	6H-SiC	2H-GaN	Diamond	2H-AlN
Bandgap (eV)	1.12	2.4	3.2	3.0	3.4	5.6	6.2
Intrinsic carrier concentration (300 K) (cm^{-3})	$1.0 \cdot 10^{10}$	6.9	$8.2 \cdot 10^{-9}$	$2.3 \cdot 10^{-9}$	$1.6 \cdot 10^{-10}$	$1.6 \cdot 10^{-27}$	$\sim 10^{-27}$
Electron mobility ($cm^{-2} \cdot V^{-1} \cdot s^{-1}$)	1400	900	1000*	400*	900	1900	135
Hole mobility ($cm^{-2} \cdot V^{-1} \cdot s^{-1}$)	600	40	115*	101*	850	1600	14
Electron saturation velocity (10^7 cm/s)	1.0	2.5	2.0	2.0	2.5	2.7	2.0
Breakdown electric field strength ($MV \cdot cm^{-1}$)	0.3	1.2	2.0	2.4	3.3	5.6	2.0
Thermal conductivity ($W \cdot cm^{-1} \cdot K^{-1}$)	1.5	3.6	4.5	4.5	1.3	2.85	20
Thermal expansion coefficient (10^{-6}/K)	2.6	3.28	3.3*	3.35*	5.59*	0.8	5.27*
Dielectric constant	11.7	9.72	9.66*	9.66*	9.0	5.5	8.5
Young's modulus (GPa)	150	748	748	748	373	1220	322

Table 1.1 Electrical, mechanical and optical properties of silicon and wide bandgap materials. (*values perpendicular to the c-axis.)

bilayer looks as hexagons and the different bilayers are depicted as shown in Figure 1.3. By different stacking orders of the bilayers, different types of SiC will form as in Figure 1.4. When the stacking order is ABCABC…, 3C-SiC is formed, which is a cubic zinc blende structure. On the other hand, the stacking order of ABABAB… will form 2H-SiC which is a hexagonal wurtzite structure. 4H-SiC has a stacking order of ABACABAC…, while the stacking order of 6H-SiC is ABCACBABCACB…. Those two have mixed structures of hexagonal and cubic [13, 14]. 4H-SiC and 6H-SiC wafers with epitaxial layers are already commercially available, while 3C-SiC can be heteroepitaxially grown on silicon wafers [15]. This is one of the advantages to use SiC for harsh environment applications.

Table 1.1 compares some wide bandgap materials and silicon in the electrical, mechanical, optical aspects for harsh environment applications [13, 14, 16]. 4H-SiC, as a

promising material for harsh environment electronics and sensing applications, has multiple advantages. For the extreme temperature electronic applications, 4H-SiC has a properly wide bandgap, low intrinsic carrier concentration at room temperature, high electron mobility, relatively high hole mobility, large electron saturation velocity and high breakdown electric field strength. It also exhibits high thermal conductivity which reduces self-heating effect and provides more accurate temperature sensing ability. It has a high Young's Modulus which is good for high pressure, high strain harsh environment applications [17]. In addition to these, 4H-SiC also has good chemical stability for the corrosive harsh environment applications. Furthermore, single crystal 6-inch 4H-SiC wafers with epi layers are commercially available. All of the above make 4H-SiC the excellent candidate for harsh environment electronic and sensing applications.

1.3 4H-SiC Extreme-temperature Low-power Applications

4H-SiC has been widely used in high-voltage high-power applications due to its high breakdown electric field, high thermal conductivity, and commercially available single crystal wafers [18, 19]. Different from its applications in power electronics, harsh environment sensing applications of 4H-SiC are aimed to extreme-temperature low-power applications. Taking its sensing applications in industrial gas turbine and geothermal well as the examples in Table 1.2, the temperature requirement is 500 ^oC and it is desirable to push it to 600 ^oC for more application purposes. Unlike the high power

Application Environment	Industrial gas turbine	Geothermal well
Operation Temperature	RT to 500 ^oC	300 ^oC ~ 400 ^oC
Electronic Requirements	Temperature: ~500 ^oC Power: ~ 0.5 W Voltage: ~ < 30 V Frequency: 50~1000 Hz	Temperature: ~ 400 ^oC Voltage: 10 ~ 20 V Frequency: 100~1000 kHz

Table 1.2 Electronic requirements for harsh environment sensing applications in industrial gas turbine and geothermal well.

applications which have thousand-volt-level voltages, the required voltages for the sensing applications are approximately 30 V and the required power is only around several Watts. The low power requirement of the sensing applications provides possibility of higher temperature operation because the self-heating is much smaller and the metallization is more stable at low power. The high power applications of 4H-SiC electronics provide 175 ^{o}C – 225 ^{o}C temperature operation [20]. For the low power applications of 4H-SiC electronics and sensors, the 4H-SiC electronics has a theoretically functional temperature of 800-900 ^{o}C for the semiconductor [21]. Taking into account the fabrication limitations, it is very possible to make the 4H-SiC electronics and sensors work at 600 ^{o}C. Therefore, our goal is to develop 4H-SiC extreme-temperature low-power electronics for harsh environment sensing applications.

1.4 Research Objective and Thesis Overview

Extreme-temperature low-power electronics and sensors that operate at 300-600 ^{o}C are useful for real-time in-situ monitoring of oil/gas exploration, geothermal well development, industrial manufacturing process, and space exploration. 4H-SiC is chosen as the suitable material for this purpose. In this dissertation, detailed research approach is described for extreme temperature performance of 4H-SiC p-n diode and its sensing application.

Chapter 2 describes the temperature-dependent coefficients of 4H-SiC and the device physics of 4H-SiC p-n diode from room to extreme temperature. In Chapter 3, the fabrication process of 4H-SiC p-n diode is depicted. In Chapter 4, the characterization of 4H-SiC p-n diode is performed from room temperature to 600 ^{o}C. Its application as a temperature sensor is described and demonstrated. Chapter 5 summarizes the contributions of this work and future research directions are suggested.

Chapter 2

Material and Device Physics from Room to Extreme Temperature

2.1 Temperature-dependent Coefficients of 4H-Silicon Carbide

For successful design of 4H-SiC extreme temperature electronic and sensing devices, it is necessary to understand the temperature-dependent coefficients of 4H-SiC material in the electrical aspect.

The energy bandgap (*Eg*) of 4H-SiC from empirical data as a function of temperature is fitted as [22]:

$$E_g = E_g(T_0) - \alpha \cdot \frac{T^2}{\beta + T} \tag{2.1}$$

where E_g (T_0) = 3.265 eV, α = 6.5×10^{-4} eV/K, β = 1.3×10^{3} K, and T is temperature in Kelvin unit. The energy bandgap of 4H-SiC as a function of temperature is plotted as in Figure 2.1. The energy bandgap slightly reduces from 3.265 eV to 3.037 eV as temperature changing from 0 K to 873 K.

The intrinsic carrier concentration (n_i) of 4H-SiC can be calculated from density of states. The intrinsic carrier concentration of 4H-SiC is as follows [23]:

$$n_i = \sqrt{N_C N_V} \cdot e^{-\frac{E_g}{2kT}} \tag{2.2}$$

$$N_C = 2M_C\left(\frac{2\pi m_e^* kT}{h^2}\right)^{\frac{3}{2}} \tag{2.3}$$

$$N_V = 2\left(\frac{2\pi m_h^* kT}{h^2}\right)^{\frac{3}{2}} \tag{2.4}$$

where N_C is the effective density of state of electrons in conduction band, N_V is the effective density of states of holes in valence band, k is Boltzmann constant, h is Planck's constant, M_C is the number of equivalent minima in the conduction band, and m_e^* and m_h^* are the density-of-states effective mass of electrons and holes, respectively. Figure 2.2

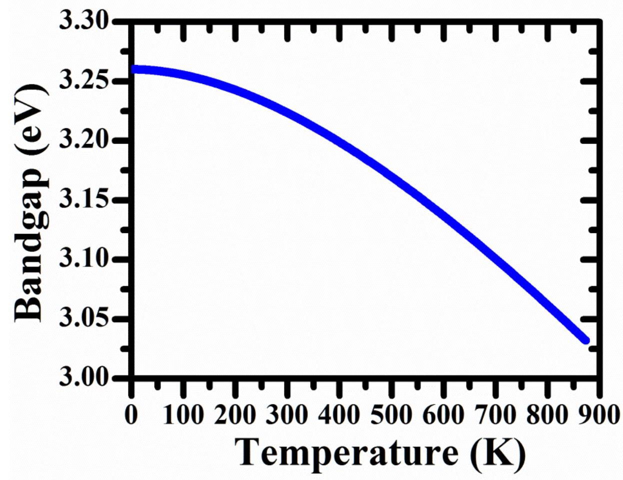

Figure 2.1 4H-SiC energy bandgap versus temperature.

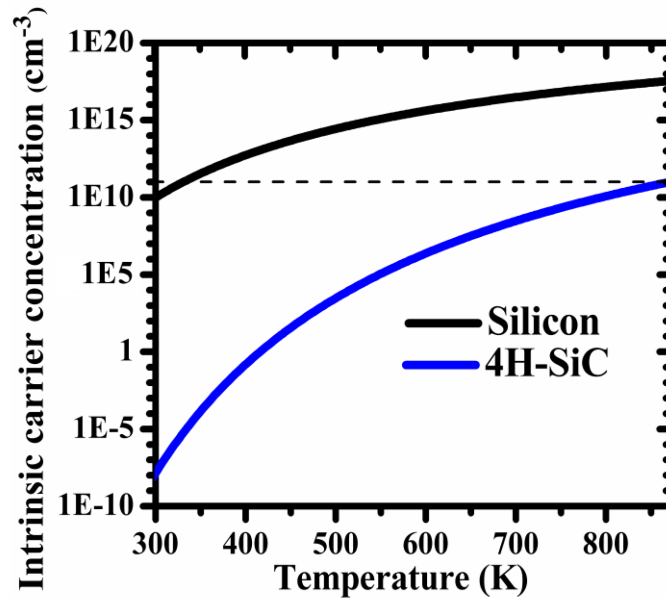

Figure 2.2 Intrinsic carrier concentrations of silicon and 4H-SiC versus temperature.

shows the relationship between temperature and the intrinsic carrier concentrations of silicon and 4H-SiC. When temperature increases from room temperature to 600 ^{o}C, the intrinsic carrier concentration of silicon goes up from 1.0×10^{10} cm^{-3} to 3.5×10^{17} cm^{-3} while the intrinsic carrier concentration of 4H-SiC rises from 8.2×10^{-9} cm^{-3} to 1.0×10^{11} cm^{-3}. We can see the intrinsic carrier concentration of 4H-SiC at 600 ^{o}C is the same with the one of silicon at 55 ^{o}C, which provides the potential of 4H-SiC operating at extreme high temperature.

2.2 Device Physics of 4H-SiC p-n Diode

As mentioned in Chapter 1, we are interested in the low-power low-voltage applications of 4H-SiC p-n diodes, on which the next discussion is focused. There are five operating ranges of 4H-SiC p-n diode in the order of the voltage bias: reverse bias range, generation-recombination range, ideal diode range, high-level injection range and series resistance range [24].

Generation-recombination happens in the depletion region and is the dominant component of current in the small reverse bias range and the first part of the forward bias range. Considering that most of the recombination happens via midgap states, the generation-recombination current is given by the following equation:

$$I_{\mathrm{G_R}} = I_g \left\{ \exp\left[\frac{qU}{\eta_1 kT} \right] - 1 \right\} \tag{2.9}$$

$$I_g = \frac{q n_i W_D A}{2\tau_{G_R}} \tag{2.10}$$

where U is the voltage that is applied across the p-n junction only, q is the absolute value of the electron charge, and η_1 is the ideality factor which is 2 for the 4H-SiC generation-recombination process. I_g is the generation current, W_D is the depletion width of the p-n diode, τ_{G_R} is the carrier generation lifetime, and A is the junction area of the diode.

At high reverse voltage, tunneling current and impact ionization current also need to be considered, as they lead to breakdown of the diode. However, in this work, we focus only on low-voltage low-power applications.

In the ideal diode (low-level injection) range, the total current is the sum of drift current and diffusion current. Deviation of the current from the ideal can be solved using Gauss's law, Poisson's equation and the continuity equation with the assumption that the

number of the minority carriers is much smaller than that of the majority carriers. The current-voltage relationship in the ideal diode range is as below:

$$I_{ID} = I_o \left\{ \exp\left[\frac{qU}{\eta_2 kT} \right] - 1 \right\} \tag{2.11}$$

$$I_o = qA \left(\sqrt{\frac{kT}{q} \frac{\mu_n}{\tau_n}} \frac{n_i^2}{N_A^-} + \sqrt{\frac{kT}{q} \frac{\mu_p}{\tau_p}} \frac{n_i^2}{N_D^+} \right) \tag{2.12}$$

where η_2 is the ideality factor which is 1 for the ideal diode range of 4H-SiC p-n diode, and I_0 is the drift current or the diffusion current at zero bias. μ_n and μ_p are the mobilities of electrons and holes, respectively. τ_n and τ_p designate the minority carrier lifetime of electrons and holes, respectively. N_A^- and N_D^+ are ionized acceptor and donor concentrations, respectively.

The high-level injection range can also be analyzed with Gauss's law, Poisson's equation and the continuity equation, but the low-level injection assumption does not stand any more. The injected minority carrier concentration is comparable with the majority carrier concentration. The high-level injection range also has an exponential current dependence of the applied voltage. The current-voltage relationship of the 4H-SiC p-n diode in the high-level injection range is as follows:

$$I_{HI} = I_{hi0} \cdot \exp\left[\frac{qU}{\eta_3 kT} \right] \tag{2.13}$$

$$I_{hi0} q = An_i \left(\sqrt{\frac{kT}{q} \frac{\mu_n}{\tau_n}} + \sqrt{\frac{kT}{q} \frac{\mu_p}{\tau_p}} \right) \tag{2.14}$$

where η_3 is the ideality factor which is 2 for the high-level injection range of 4H-SiC p-n diode, and I_{hi0} is a constant current value as in Equation 2.14.

When the applied voltage on the 4H-SiC p-n diode goes well beyond the turn-on voltage, the current won't increase exponentially anymore because the effect of series resistance will become significant, and the current will increase linearly as the voltage continues going up. The current-voltage relationship of the 4H-SiC p-n diode in the series resistance range is given by:

$$V = V_{th} + I \cdot R \tag{2.15}$$

where V_{th} is the turn-on voltage of the 4H-SiC p-n diode, and R is the series resistance. The slope of the I-V curve in the series resistance range is 1/R.

In the previous ranges we have discussed, even if the current is exponentially dependent on the voltage applied across the p-n junction, the series resistance is still involved in the total applied voltage as follows:

$$V = U + I \cdot R \Rightarrow U = V - I \tag{2.15}$$

where V is the total applied voltage. Substituting U with $V\text{-}I{\cdot}R$ in Equations (2.9), (2.11) and (2.13), we are able to obtain the relationships of the total voltage and current in the low reverse range, generation-recombination range, the ideal diode range and the high-level injection range.

In the depletion region of the 4H-SiC p-n diode device, generation-recombination, drift and diffusion processes occur at the same time, while in 4H-SiC p-n diode with $I_g >> I_0$, the generation-recombination process dominates in the low reverse voltage range and the low forward voltage range. When the forward bias increases, the depletion width decreases, so the generation-recombination current is negligible and diffusion current dominates. Therefore, we can write those two together in the following [8]:

$$I = I_g \left\{ \exp\left[\frac{q(V - I \cdot R)}{\eta_1 kT} \right] - 1 \right\} + I_o \left\{ \exp\left[\frac{q(V - I \cdot R)}{\eta_2 kT} \right] - 1 \right\} \tag{2.16}$$

This is the full expression of the current-voltage relationship of the 4H-SiC p-n diode. This model takes into account the generation-recombination, drift, diffusion, and series resistance in the 4H-SiC p-n diode, which is able to predict the performance of a 4H-SiC p-n diode very well. We can derive from Eq. (2.10), (2.12) and (2.16) that the current will increase greatly with increasing temperature. Here the high-level injection effect is not taken into account since it is just a different case for the drift and diffusion current and it might be negligible in some devices.

Figure 2.3 shows the simulated current-voltage plots of 4H-SiC p-n diode from room temperature to 600 °C. The temperature dependences of energy bandgap, intrinsic carrier concentration, carrier mobilities of electrons and holes, ionization degrees of different doping levels, recombination-generation and parasitic resistances are considered in this model. The turn-on voltage of the 4H-SiC p-n diode changes from 2.7 V to 1.4 V as the temperature increases from 17 °C to 600 °C with the average shifting rate of 2.22 mV/ ºC. The on-resistance of the 4H-SiC p-n diode varies from 1.85 kΩ to 0.48 kΩ as the temperature increases from 17 °C to 600 °C with the average changing rate of 2.35 Ω/ ºC.

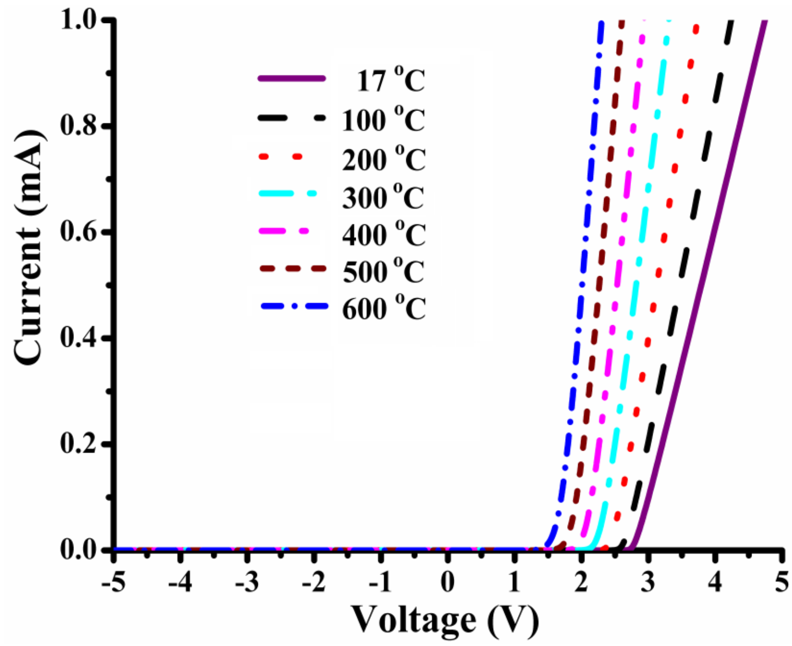

Figure 2.3 The simulated current-voltage plots of 4H-SiC p-n diode from room temperature to 600 °C.

Chapter 3

Fabrication of 4H-SiC p-n Diode

3.1 Fabrication Process of 4H-SiC p-n Diode

The starting wafer is depicted in Figure 3.1. There are four epitaxial layers (from Ascatron AB) on top of a single crystal 4H-SiC substrate (from Cree Inc.). The first epitaxial layer is a 0.5 μm p^+ layer with an aluminum dopant concentration of 6×10^{18} cm^{-3}. The second epitaxial layer is a 1 μm n-type layer with a nitrogen dopant concentration of 1×10^{17} cm^{-3}. These two layers form the p-n junction for the 4H-SiC p-n diode. The third epitaxial layer is a 1 μm n^+ layer with a nitrogen dopant concentration of 3×10^{19} cm^{-3}, which is used for a better ohmic contact with metal. The fourth epitaxial layer is a 3 μm p^- layer with an aluminum dopant concentration of 1×10^{15} cm^{-3}, which forms another p-n junction for device isolating purpose.

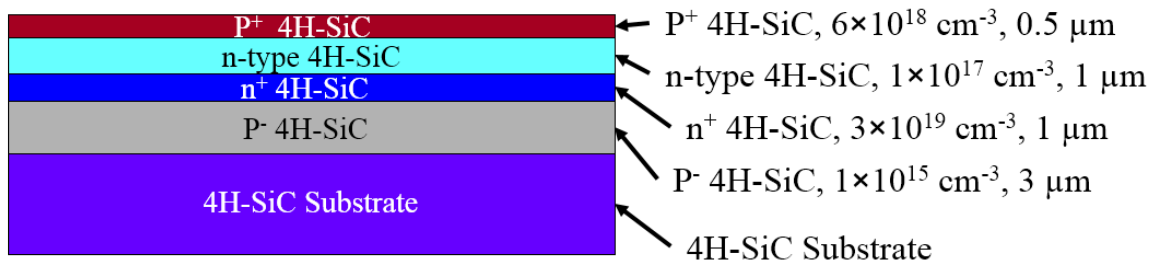

Figure 3.1 Starting wafer for the 4H-SiC p-n diode fabrication process.

Figure 3.2 comprises a top-view schematic and a cross-sectional view schematic of a 4H-SiC p-n diode in this work. Both of the metal contacts are on the top surface of the wafer for further planar integration purpose. The circularly shape p-n junction enables the elimination of the corner effect *i.e.* the higher electrical field near the rectangular corners. Three diameters are chosen as 100 μm, 200 μm and 500 μm. Figure 3.2 (a) also lists the

masks for the fabrication process in the following order: the bottom contact exposing mask, the device isolation mask, the passivation patterning mask, the n-type metal mask and the p-type metal mask.

The fabrication process of the 4H-SiC p-n diode is depicted in Figure 3.3. The two columns of each sub-item in Figure 3.3 represent the cross-section after each fabrication step and the top view of the layout design of the 4H-SiC p-n diode, respectively. The fabrication process is begun with the 4H-SiC starting wafer with four epitaxial layers. The first step is a transformer coupled plasma (TCP) 4H-SiC etching step with silicon oxide as a hard mask to expose the n^+ contact layer. This step also defines the p-n junction of the 4H-SiC diode. The second step involves another TCP 4H-SiC etching step to isolate single diodes. The third step is plasma enhanced chemical vapor deposition

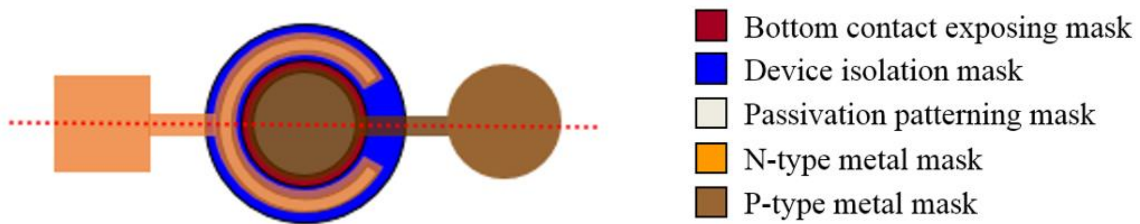

(a)

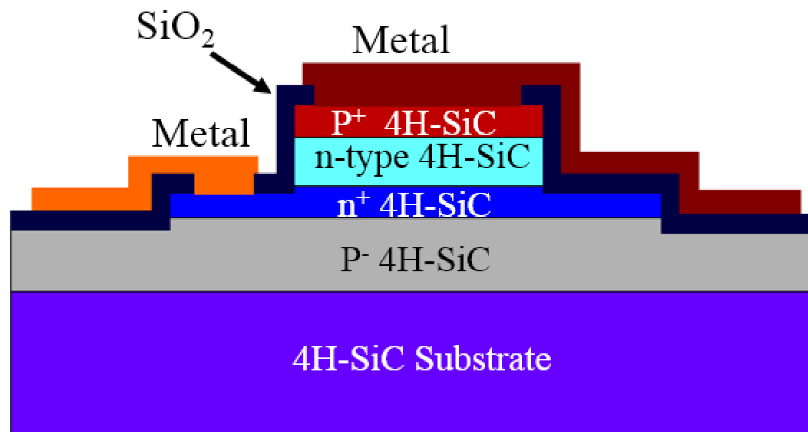

(b)

Figure 3.2 (a) Top view schematic of the 4H-SiC p-n diode; (b) cross-sectional view schematic of the 4H-SiC p-n diode along the red line in (a).

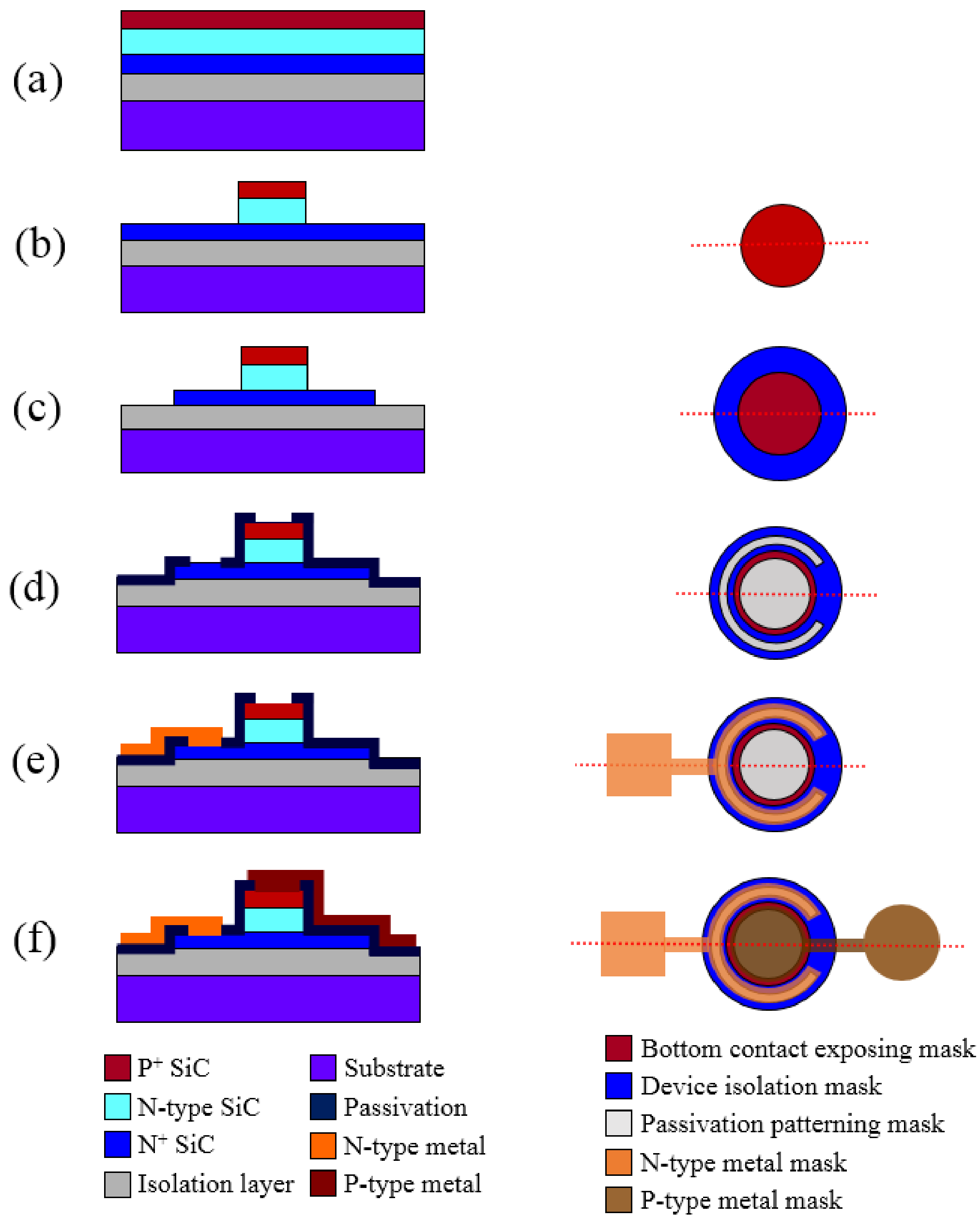

Figure 3.3 (a) Starting wafer: single crystal 4H-SiC wafer with four epitaxial layers; (b) first SiC etching to expose the n^+ contact layer; (c) second SiC etching to isolate single diode; (d) oxide passivation deposition and patterning; (e) n-type metal liftoff and annealing; (f) p-type metal liftoff and annealing.

(PECVD) of silicon oxide which is employed as a passivation layer. The fourth step is sputtering n-type metal contact which is Ni/Ti and defining the pattern by liftoff process. A rapid thermal annealing (RTA) step is followed to form ohmic contact. The fifth step is sputtering p-type metal contact which is Al/Ti/Ni and patterning it by liftoff. A RTA step is next to form ohmic contact [25].

3.2 Fabricated 4H-SiC p-n Diode and Characterization Platform

The optical microscopic image of the fabricated 4H-SiC p-n diode is presented in Figure 3.4. This diode has a circular junction with 200 μm diameter. The square metal pad is connected to p-type electrode of the 4H-SiC p-n diode and the circular metal pad is connected to n-type electrode of the diode.

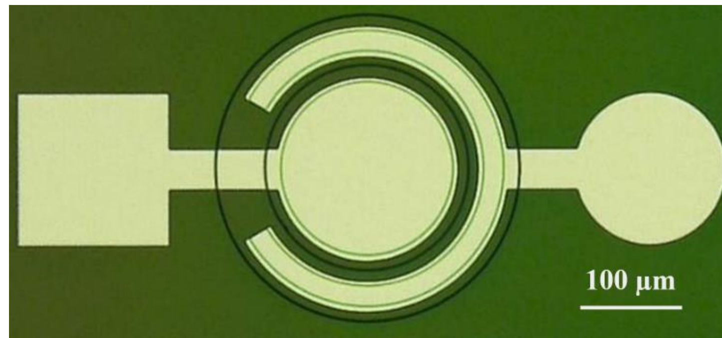

Figure 3.4 The optical microscopic image of the fabricated 4H-SiC p-n diode with a 200 μm diameter circular junction.

The 4H-SiC p-n diodes are characterized with a high temperature probe station (from Signatone Inc.) as shown in Figure 3.5. The high temperature probe station consists of eight probe arms, a ceramic hot chunk, a microscope, a thermal heater, and a water cooler. The probe arms, the ceramic hot chunk and the microscope are placed in a black box on a vibration isolation table. The ceramic hot chunk can be stably heated up to 600 ^{o}C within ±1 ^{o}C variation. The system has low thermal current noise which is in pico-amperes at room temperature and in nano-amperes at 600 ^{o}C. An Agilent B2912A precision source measurement unit is used to test the current-voltage curve. The

fabricated chip was placed on the hot chunk. Two probes were placed in contact with the p-type and n-type electrodes of the p-n diode and then connected to the source measurement unit. I-V curve was measured at different temperature from room temperature to 600 ^{o}C with this characterization platform.

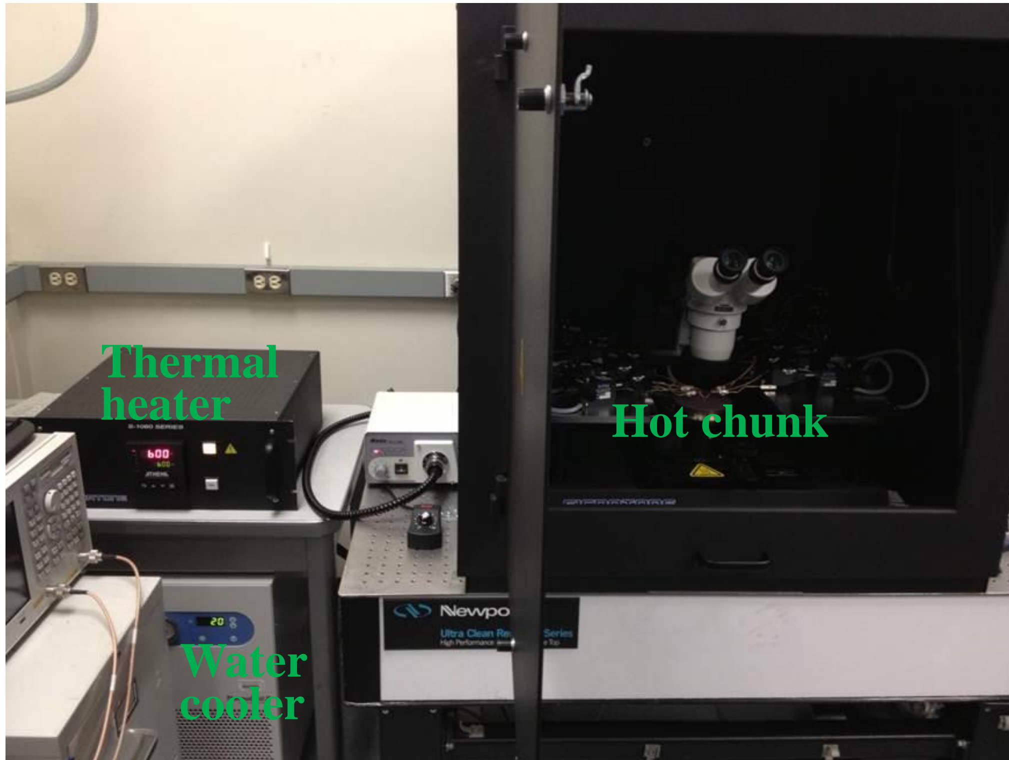

Figure 3.5 The high temperature probe station including hot chunk, thermal heater, and water cooler.

Chapter 4

Device Performance and Temperature Sensing Applications of 4H-SiC p-n Diode

4.1 Device Performance of 4H-SiC p-n Diode from Room to Extreme Temperature

Figure 4.1 shows the tested current-voltage characteristics of the 4H-SiC p-n diode from room temperature to 600 ºC. The I-V curve shifts from right (large voltage) to left (small voltage) in Fig. 4.1 when the temperature increases. The turn-on voltages of the fabricated 4H-SiC p-n diode decreases from 2.6 V to 1.3 V when temperature increases from room temperature to 600 ºC, with a shifting rate of 2.2 mV/ºC. The on-resistance of the 4H-SiC p-n diode varies from 2.1 kΩ to 0.5 kΩ as the temperature increases from 17 °C to 600 °C with the average changing rate of 2.8 Ω/°C. This is in good agreement with the simulation results in Figure 2.3.

Figure 4.2 is the tested current-voltage curves of the 4H-SiC p-n diode from room temperature to 600 ºC in a semi-log plot. In this figure, we are able to see the different operating voltage ranges of the 4H-SiC p-n diode, which were discussed in Section 2.2. In the low bias voltage range of each I-V curve, the ideality factor is approximately 2, which corresponds to the generation-recombination range of the 4H-SiC p-n diode. The slope becomes smaller with temperature increasing due to the q/2kT factor in Eq. (2.9). The shift of the curve with temperature is very uniform in this range.

As voltage goes larger, the I-V curves shift to the ideal diode range and the ideality factor is approximately 1 as in Eq. (2.11). The higher temperature curves have better fitting in this range because the series resistance is smaller and has smaller influence on the curve.

When voltage bias is larger than the turn-on voltage, the slope becomes much

smaller than the previous ranges and series resistance dominates. The slope is the reciprocal of the on-resistance.

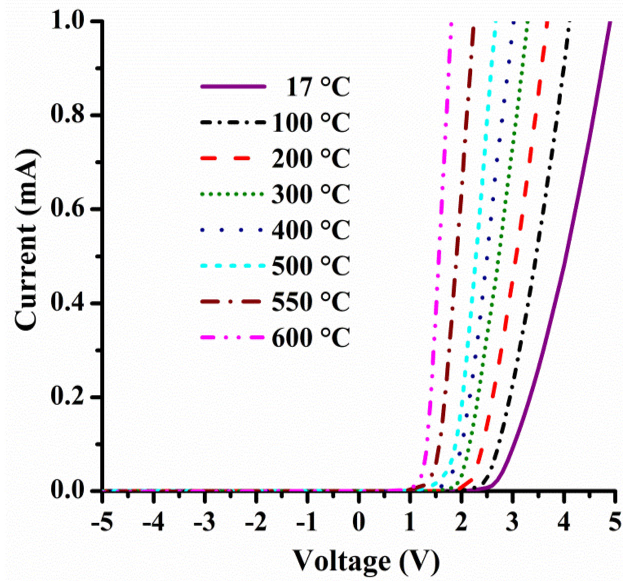

Figure 4.1 The testing results of 4H-SiC p-n diode from room temperature to 600 ºC.

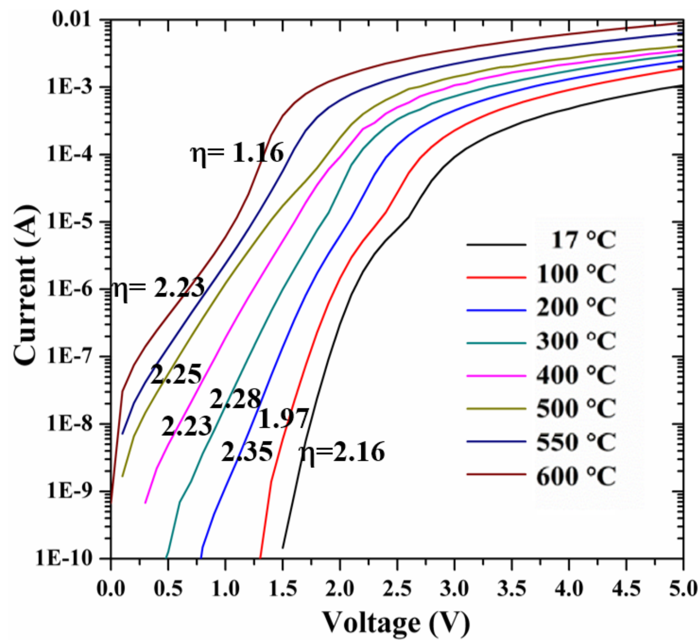

Figure 4.2 The testing results of 4H-SiC p-n diode from room temperature to 600 ºC in a semi-log plot.

Figure 4.3 compares the simulated and experimental results of the 4H-SiC p-n diode from room temperature to 600 ºC. Figure 4.3 (a) is the comparison of turn-on voltage and Figure 4.3 (b) is the comparison of the on-resistance. The experimental results are in good agreement with the simulating results with small deviations. The difference could come from the defects of the 4H-SiC material and the fabrication processes.

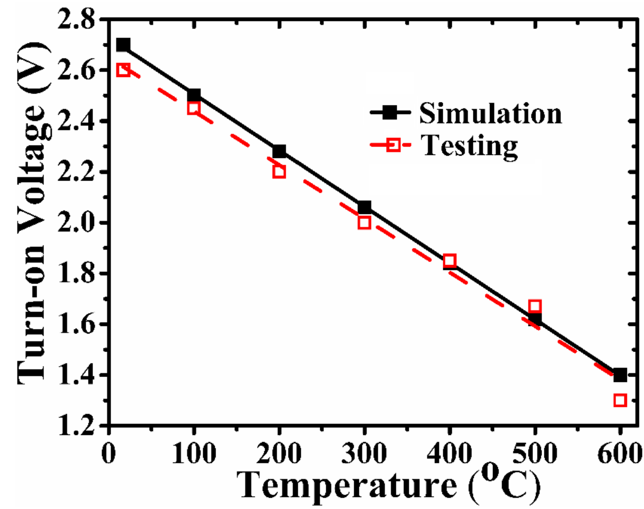

(a)

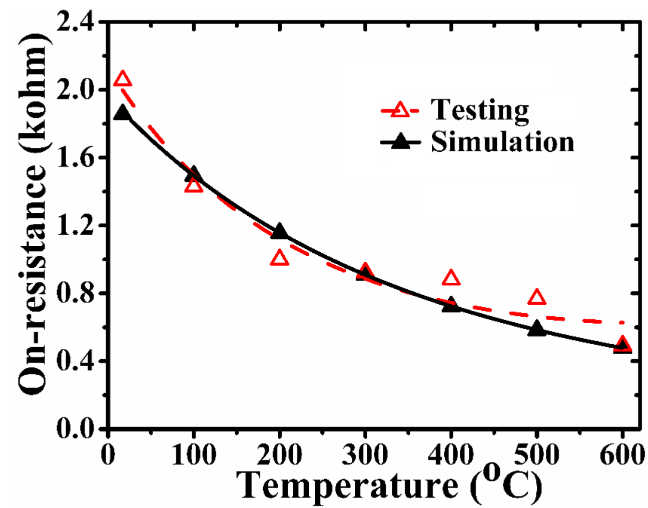

(b)

Figure 4.3 Comparison of the simulation and testing results of the 4H-SiC p-n diode from room temperature to 600 ºC. (a) Comparison of turn-on voltage; (b) comparison of the on-resistance.

4.2 Temperature Sensing Applications of 4H-SiC p-n Diode

Our goal is to use the 4H-SiC p-n diode for harsh environment sensing applications as mentioned in Chapter 1. We have discussed the electrical properties of the 4H-SiC p-n diode in the previous chapters. Now it is necessary to discuss its sensing applications in harsh environment. One good example of 4H-SiC p-n diode used in harsh environment sensing applications is as a temperature sensor.

As we demonstrated in Section 4.1, the fabricated 4H-SiC p-n diode can survive as high as 600 ^{o}C. Compared to SiC Schottky diode temperature sensors which were reported to be functional up to 400 ^{o}C [26], the sensing temperature range is much larger. Therefore, 4H-SiC p-n diode is a very promising candidate to be used as an extreme high temperature sensor.

The working principle of the temperature sensing application of a p-n diode is based on its high temperature dependence of its current-voltage relationship in Eq. (2.16). Figure 4.4 and Figure 4.5 demonstrates the temperature sensing application of the fabricated 4H-SiC p-n diode. At 1 mA current, the 4H-SiC p-n diode temperature sensor has a high sensitivity of 4.72 mV/^{o}C as in Fig. 4.4. At 0.1 μA current, the sensitivity of

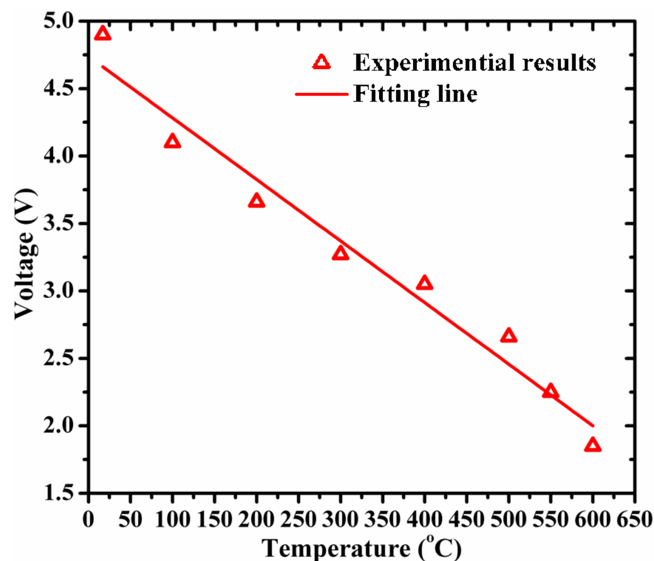

Figure 4.4 The temperature sensing demonstration of 4H-SiC p-n diode from room temperature to 600 ^{o}C at 1 mA current.

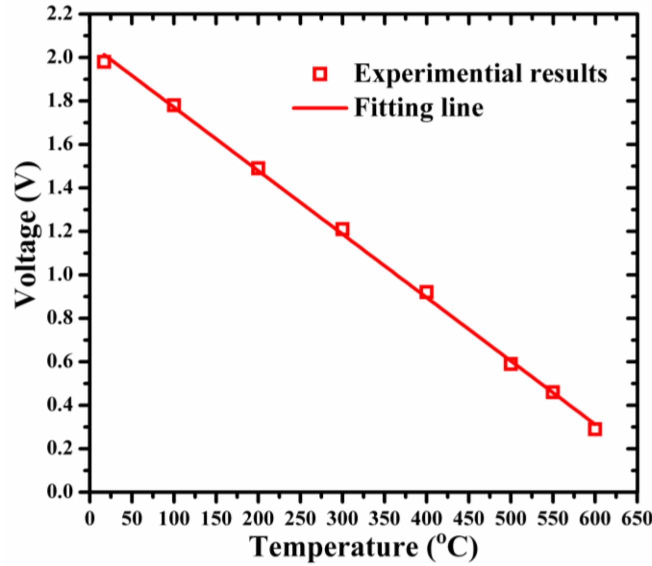

Figure 4.5 The temperature sensing demonstration of 4H-SiC p-n diode from room temperature to 600 °C at 0.1 μA current.

the 4H-SiC p-n diode temperature sensor is 2.92 mV/°C as shown in Fig. 4.5. Though the sensitivity is lower, it has a better sensing linearity. Thus, when employing the 4H-SiC p-n diode as a temperature sensor, you can choose corresponding current value based on your application requirements.

Chapter 5

Conclusion and Future Work

5.1 Conclusion

In this work, we demonstrate the stable operation of 4H-silicon carbide (SiC) p-n diodes at temperature up to 600 ºC. The application background, the material and device physics, the fabrication process, the characterization and the temperature sensing application of the 4H-SiC p-n diode are described. The simulation results indicate that the turn-on voltage of the 4H-SiC p-n diode changes from 2.7 V to 1.4 V as the temperature increases from 17 ºC to 600 ºC. The on-resistance of the 4H-SiC p-n diode varies from 1.85 kΩ to 0.48 kΩ as the temperature increases from 17 °C to 600 °C. The turn-on voltages of the fabricated 4H-SiC p-n diode decreases from 2.6 V to 1.3 V when temperature changes from 17 ºC to 600 ºC. The on-resistance of the 4H-SiC p-n diode varies from 2.1 kΩ to 0.5 kΩ as the temperature increases from 17 °C to 600 °C. The experimental I-V curves of the 4H-SiC p-n diode from 17 ºC to 600 ºC agree with the simulation model we built. The demonstration of the stable operation of the 4H-SiC p-n diodes at high temperature up to 600 ºC brings out great potentials for 4H-SiC devices and circuits working in harsh environment electronic and sensing applications.

5.2 Future Work

There are several topics that need to be further studied. In order to fully understand the temperature dependences of the 4H-SiC p-n diodes, more temperature-dependent coefficients need to be taken into account. The metal contacts for both p-type and n-type 4H-SiC and a robust interconnect should also draw our attention for stable high temperature operation. Further characterization of the 4H-SiC p-n diodes can be done for better comprehensive study of the device performance.

Meanwhile, p-n diode is also the basic structure for some transistors such as junction gate field-effect transistor (JFET) and bipolar junction transistor (BJT). Further study can be extended to the transistors. There are multiple applications of the 4H-SiC p-n diodes besides temperature sensing which can be explored. At last but not least, since we designed both of the contacts on the front surface of the wafer, some planar integrated circuits based on 4H-SiC p-n diodes can be formed and studied for more harsh environment electronics and sensing applications.

References

[1] X. Gong, L. An, and C. Xu, "Wireless passive sensor development for harsh environment applications," in *2012 IEEE International Workshop on Antenna Technology (iWAT)*, 2012, pp. 140-143.

[2] http://www.energy.siemens.com/

[3] M. Mehregany, "Advances in silicon carbide micro-and nano-electro-mechanical systems fabrication technology and applications," in *2013 Transducers & Eurosensors XXVII: The 17th International Conference on Solid-State Sensors, Actuators and Microsystems (TRANSDUCERS & EUROSENSORS XXVII)* , 2013, pp. 2397-2402.

[4] N. A. Riza, M. Sheikh, and F. Perez, "Hybrid wireless-wired optical sensor for extreme temperature measurement in next generation energy efficient gas turbines," *Journal of Engineering for Gas Turbines & Power,* vol. 132, p. 051601, 2010.

[5] P. R. Ohodnicki, M. Buric, and S. Seachman, "Functional sensor material enabled harsh environment, high temperature optical sensors for energy applications," *Sensors for Extreme Harsh Environments II*, 9467-53, 2015.

[6] D. G. Senesky, B. Jamshidi, K. B. Cheng, and A. P. Pisano, "Harsh environment silicon carbide sensors for health and performance monitoring of aerospace systems: A review," *IEEE Sensors Journal,* vol. 9, pp. 1472-1478, 2009.

[7] S. Shao, W.-C. Lien, A. Maralani, and A. Pisano. “Integrated 4H-Silicon Carbide Diode Bridge Rectifier for High Temperature (773 K) Environment.” 44th European Solid State Device Research Conference (ESSDERC), pp. 138-141, 2014.

[8] S. Shao, W.-C. Lien, A. Maralani, J. Cheng, K. Dorsey, and A. Pisano. “4H-Silicon Carbide p-n Diode for High Temperature (600 °C) Environment Applications.” European Conference on Silicon Carbide & Related Materials (ECSCRM), 2014.

[9] W.-C. Lien, D.-S. Tsai, S.-H. Chiu, D. Senesky, R. Maboudian, A. Pisano, and J.-H. He, "Nanocrystalline SiC metal-semiconductor-metal photodetector with ZnO nanorod arrays for high-temperature applications," in *2011 16th International*

Solid-State Sensors, Actuators and Microsystems Conference (TRANSDUCERS), 2011, pp. 1875-1878.

[10] P. G. Neudeck, R. S. Okojie, and L.-Y. Chen, "High-temperature electronics-a role for wide bandgap semiconductors?," *Proceedings of the IEEE,* vol. 90, pp. 1065 -1076, 2002.

[11] M. R. Werner and W. R. Fahrner, "Review on materials, microsensors, systems and devices for high-temperature and harsh-environment applications," *IEEE Transactions on Industrial Electronics,* vol. 48, pp. 249-257, 2001.

[12] F. Goericke, K. Mansukhani, K. Yamamoto, A. Pisano. "Experimentally validated aluminum nitride based pressure, temperature and 3-axis acceleration sensors integrated on a single chip." *Micro Electro Mechanical Systems (MEMS), 2014 IEEE 27th International Conference on*. IEEE, 2014.

[13] C.-M. Zetterling, *Process technology for silicon carbide devices*: IET, 2002.

[14] W.-C. Lien. "*Porous and Epitaxial 3C-SiC Thin Films Technology for Micro-electromechanical Systems and Electronics Applications*," Dissertation, University of California, Berkeley, 2008.

[15] W.-C. Lien, N. Ferralis, C. Carraro, and R. Maboudian, "Growth of epitaxial 3C-SiC films on Si (100) via low temperature SiC buffer layer," *Crystal Growth & Design,* vol. 10, pp. 36-39, 2009.

[16] C.-M. Lin, "*Temperature-Compensated and High-Q Piezoelectric Aluminum Nitride Lamb Wave Resonators for Timing and Frequency Control Applications*," Dissertation, University of California, Berkeley, 2013.

[17] S. Wodin-Sshwartz, "*MEMS Materials and Temperature Sensors for Down Hole Geothermal System Monitoring*," Dissertation, University of California, Berkeley, 2013.

[18] D. Peftitsis, G. Tolstoy, A. Antonopoulos, et al, "High-power modular multilevel converters with SiC JFETs." *Power Electronics, IEEE Transactions on,* 27(1), 28-36, 2012.

[19] Tiwari, Sunita, et al. "Silicon carbide power transistors, characterization for smart grid applications." *15th International IEEE Power Electronics and Motion Control Conference (EPE/PEMC),* 2012.

[20] Z. Chen, Y. Yao, M. Danilovic, et al. "Performance evaluation of SiC power MOSFETs for high-temperature applications." *15th International IEEE Power Electronics and Motion Control Conference (EPE/PEMC),* 2012.

[21] K. H. J. Bushchow, R. W. Cahn, M. C. Flemings, B. Ilschner, E. J. Kramer, S. Mahajan, and P. Veyssiere Eds., *Encyclopedia of Materials: Science and Technology*, New York: Elsevier, 2001.

[22] M. E. Levinshtein, S. L. Rumyantsev, and M. S. Shur, *Properties of Advanced Semiconductor Materials: GaN, AIN, InN, BN, SiC, SiGe*: Wiley, 2001.

[23] T. Ayalew, "*SiC Semiconductor Devices Technology, Modeling, and Simulation*," Technical University of Vienna, 2004.

[24] Sze, S. M. and Ng, K. K. "*Physics of semiconductor devices*." John Wiley & Sons, 2006.

[25] Konishi, Ryohei, et al. "Development of Ni/Al and Ni/Ti/Al ohmic contact materials for p-type 4H-SiC." *Materials Science and Engineering: B* 98.3 (2003): 286-293.

[26] G Brezeanu, F Draghici, F Craciunioiu, et al. "4H-SiC Schottky diodes for temperature sensing applications in harsh environments." *Materials Science Forum*. Vol. 679. 2011.